ICANS-XIV
14th Meeting of the International Collaboration on Advanced Neutron Sources
June 14-19, 1998
Starved Rock Lodge, Utica, Illinois, USA

Ring Developments Relevant to Short-Pulse Spallation Neutron Sources

Robert J. Macek

Los Alamos National Laboratory
LANSCE-DO
MS-H848
Los Alamos NM, 87545, USA

ABSTRACT

Recent developments on major design and performance issues in the circular accelerator drivers for short-pulse spallation neutron sources are reviewed.

1. Introduction

The demand for higher intensity short-pulse spallation neutron sources has stimulated work on the intensity limitations of the circular accelerator drivers. It has also lead to a number of proposals for new facilities and upgrades to existing facilities. The two main options for new facilities are the linac plus rapid cycling synchrotron (RCS) option and the linac plus accumulator (compressor) ring option. Both make use of multi-turn injection obtained by stripping H^- beam in the injection region of the ring. Both are subject to many of the same limiting factors - space charge, beam losses and instabilities - but to differing degrees.

Both options are possible contenders for the next generation spallation sources. The RCS has the advantage that injection losses occur at a lower energy and therefore cause less radio-activation per lost proton. It has the disadvantage that the space charge limit at injection is more severe. The linac-accumulator ring has the advantage of a significantly higher space charge limit and of providing all of acceleration and beam power in a rf linac. Its main drawback is that beam losses in the ring all occur at the final energy with the consequence that there is greater induced activation per lost proton. At this time, the major new "green field" projects have tilted towards the linac-accumulator ring option but not for any single reason.

Numerous recent advances in the science and technology of circular accelerators deserve mention. However, it is not the purpose of this paper to provide a complete and exhaustive review. Instead, topics were selected that were judged of particular importance to the new machines and to the ISIS and PSR upgrades. Of prime importance are the advances made in the understanding and amelioration of the factors that limit intensity especially space charge, beam losses and instabilities. Other selected topics include stripper foil heating and foil lifetime considerations, new ideas for injection without foils (laser-aided injection), and inductive inserts for passive compensation of longitudinal space charge.

2. Limitations from Transverse Space Charge

The transverse space charge limit is one of the first constraints to consider in ring design. By now, it is a classic "text book" limit on intensity and is due to the defocusing effect of space charge which depresses the betatron tunes of individual beam particles. The simplest model that can be calculated analytically i.e. a proton oscillating inside a uniform beam distribution of circular cross section, will illustrate the essential features. In this approximation the tune shift or more precisely the incoherent tune shift, $\Delta\nu$, is given by equation (1) below:

$$(1)\quad \Delta\nu = -\frac{r_p N}{2\pi\beta^2\gamma^3\varepsilon B_f}$$

Here N is the number protons in the ring, r_p the classical radius of the proton, β and γ the usual relativistic factors, ε the transverse emittance and B_f the longitudinal bunching factor. From this formula it is apparent that the tune shift is largest at the injection energy because of the $\beta^2\gamma^3$ term in the denominator. The tune shift also depends on beam size through the emittance. A larger beam size results in a larger emittance and, therefore, a smaller tune shift.

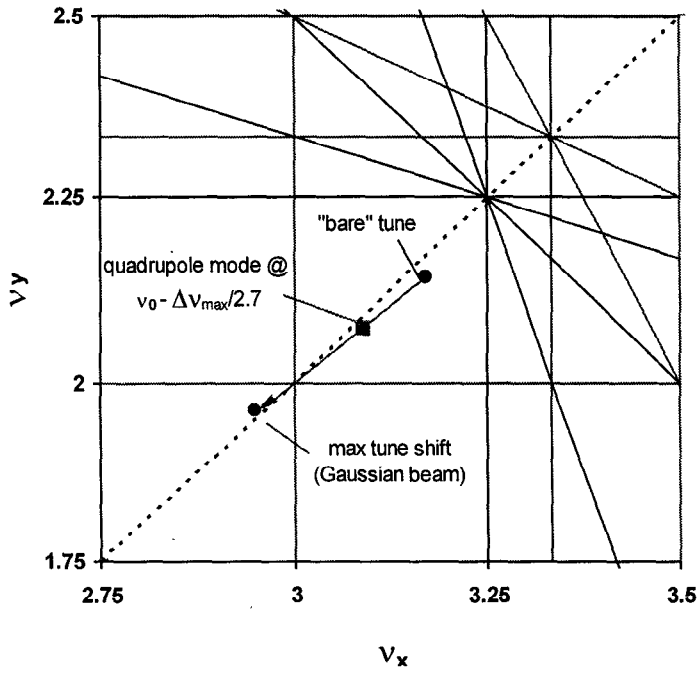

Figure 1. PSR betatron tune space diagram

The standard design criterion has been to avoid incoherent tune shifts that depress the tune over low order betatron resonances especially the integer, 1/2 integer or 1/3 integer lines. Thus, designers strive to keep $-\Delta\nu_{max} \leq \sim 0.25$. This criterion has been exceeded in a number of operating machines as the intensity was pushed up. For example, ISIS operates with a tune shift of ~ -0.4, the AGS ~-0.58 and at PSR the maximum incoherent tune shift moves the tune across the integer resonance (see Figure 1).

The reasons for being able to cross integer and half integer resonances are now better and more widely understood as was made clear by Rick Baartman at the recent Shelter Island Workshop [1]. The standard criterion is too conservative. Beam losses from space charge require consideration of collective modes and envelope oscillations. For example, with a Gaussian beam, the quadrupole mode (a low order collective mode) is not resonant until the maximum incoherent tune shift is 2.7 times that which moves the tune across the integer (see Figure 1). Higher order modes are resonant closer to the maximum tune shift.

Intensity-dependent emittance growth, presumably due to space charge, has been observed at several accelerators. Data from PSR, shown in Figure 2, illustrate the effect. In Figure 2, beam profiles at extraction are plotted for two different injection configurations, the standard injection

set up and one that produces a smaller initial beam size in the ring. For each configuration, profiles for 3 different intensities are shown. Intensity is varied in steps of a factor of 2 by changing the number of injected pulses using the front end beam chopper which can be commanded to let through every nth pulse (given by the countdown parameter, CD). Thus, for CD=1 every pulse gets through, CD =2 every other pulse and CD=4 every 4th pulse.

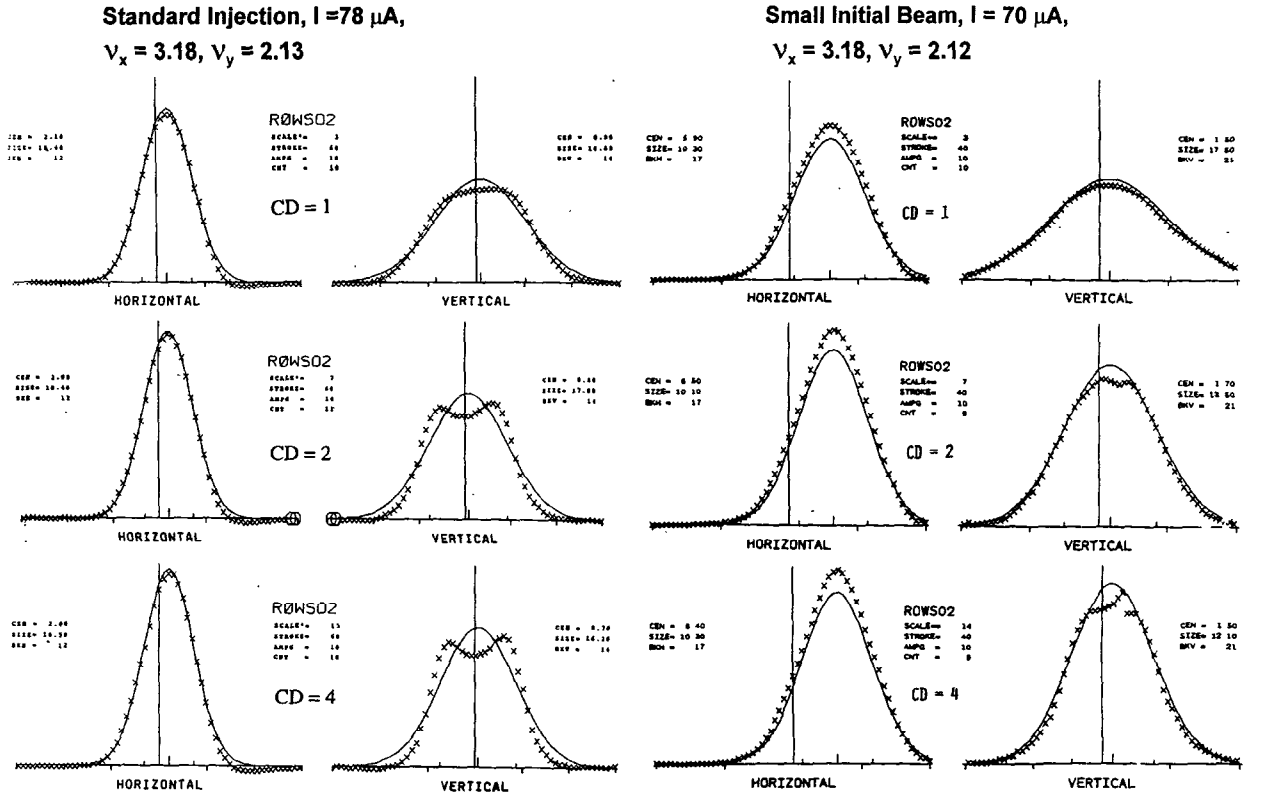

Figure 2. Beam sizes at various intensities in PSR.

The profiles of Figure 2 show that the beam emittance (proportional to the square of the beam size) increases with intensity, particularly in the vertical plane. The effect is more pronounced for the configuration with the smaller initial emittance. Here the vertical emittance increases by a factor of 1.7 for a factor of 2 change in intensity (CD=2 to CD=1).

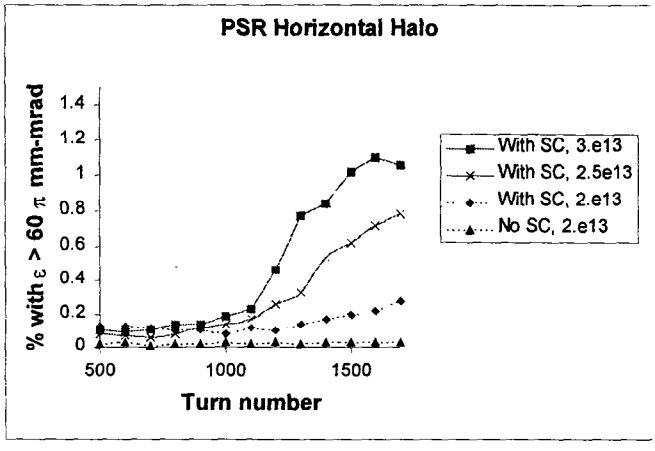

Figure 3. PIC calculations of beam halo with and without space charge.

Computation of emittance growth is a difficult problem since space charge is fundamentally a many body problem that would require enormous computing capability to treat exactly. Nevertheless, considerable progress has been made in numerical simulations as was brought out at the Shelter Island Workshop [2]. For example, the ORNL group has carried out computations of beam halo produced by space charge in the 1998 PSR using a

particle-in-cell (PIC) code [3]. Results of their calculations for PSR are shown Figure 3. These show details of the growth of emittance halo as the accumulation proceeds and as the final intensity increases. This behavior is in qualitative agreement with the experience at PSR. More quantitative comparisons are planned for the future.

With the constant demand to increase intensity, there is great interest in measures to increase the space charge limit. From equation (1) it is apparent that increasing the injection energy, increasing the longitudinal bunching factor and increasing the emittance will decrease the tune shift hence raise the space charge limit. The accumulator rings capitalize on having the highest injection energy for a given final energy. Improving the longitudinal bunching factor by adding dual harmonic rf is a feature of the new machines and a key feature of ISIS and PSR upgrades. The ISIS dual harmonic upgrade is expected to raise the intensity to 300 μA from the present 200 μA while keeping the losses constant. For PSR a second harmonic buncher will improve the bunching factor by 40% (0.5 from 0.35).

The new rings proposed for SNS, ESS, SNF (5 MW spallation neutron facility proposed for JAERI) and JHF are designed to have large transverse acceptance thereby allowing large emittances and thus smaller tune shifts. A comparison of emittance and calculated tune shifts for several rings are given in Table I below.

Table I. Comparison of emittance and maximum tune shift for several facilities.

Ring	ε (π mm-mrad)	$-\Delta\nu_{max}$
PSR 97	27- 39 (95%)	0.22
SNS	120	0.2
ESS	120	0.1
SNF	200	0.1
JHF	214	0.36

3. Beam Losses from Foil Scattering

The stripper foil is a major cause of losses for accumulator rings. Foil scattering and field stripping of excited states of H^0 produced in the foil are leading beam loss mechanisms. Stored beam particles are lost when undergoing nuclear or large angle Coulomb scattering in traversing the stripper foil. The beam loss depends on the number of foil hits, the foil thickness and the probability that the scattered particle is lost from the ring acceptance. Mitigation can be achieved by reducing the foil hits, increasing the acceptance for Coulomb scattered beam, using collimators to control the location of beam losses and by minimizing the foil thickness. The foil thickness is a trade-off with other criteria such as the amount of neutral beam that can be allowed go to the waste beam dump and minimizing the production of excited states of H^0.

The experience with PSR illustrates the problem of beam loss from foil scattering and means to reduce it. The important features of injection for PSR in 1997 operations are depicted in Figure 4 where the transverse phase space at the stripper foil is shown. The foil hits, hence beam losses from scattering, for this configuration are high ~ 300/protron or 35% chance per turn. The foil

hits are high because of certain disadvantages of H^0 injection. First, there is a factor of ~3 in emittance growth of the H^0 beam in the bend plane of the stripper magnet that creates the H^0 from H^-. Second, there is a large mismatch of the H^0 to the acceptance ellipse of the ring that exacerbates the inability to manipulate or tailor a neutral beam for optimum filling ("painting") of transverse phase space for minimum foil hits.

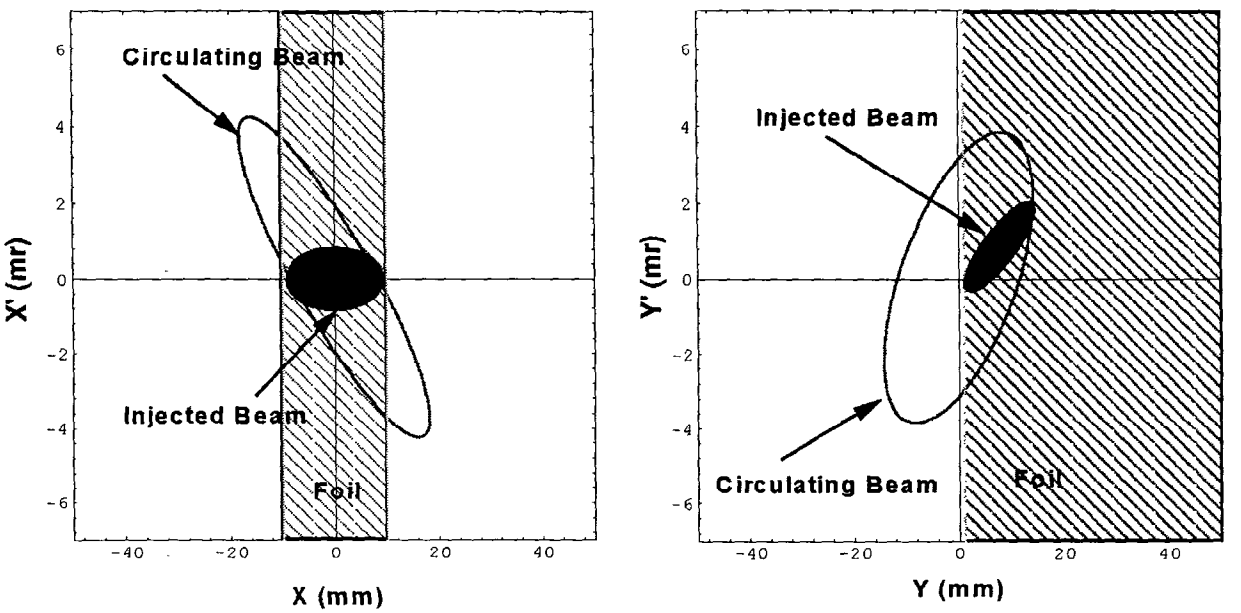

Figure 4. Transverse phase space at the foil for H^0 injection at PSR in 1997.

The upgrade to direct H^- injection depicted in Figure 5 is expected to reduce the foil hits by a factor of 10. This is accomplished by using double offset injection with a programmed closed orbit bump in the vertical plane at the foil.

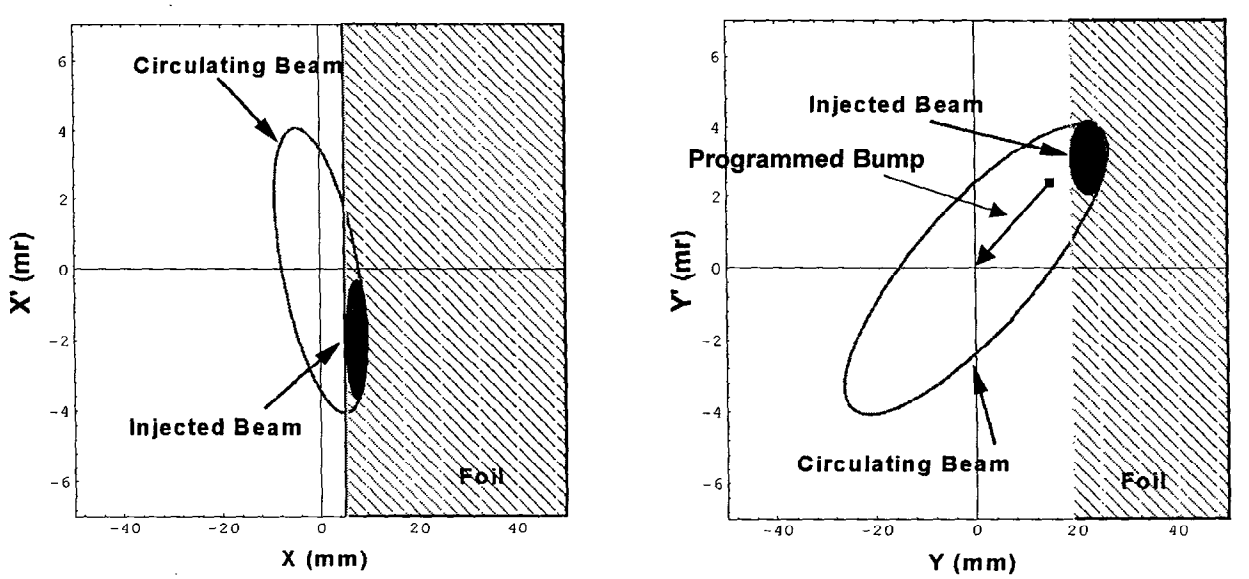

Figure 5. Transverse phase space at the stripper foil for the direct H^- upgrade to PSR.

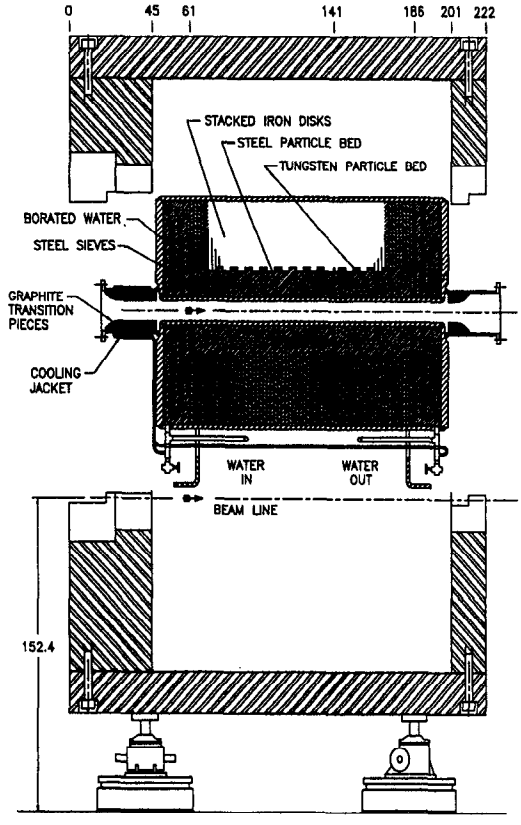

Figure 6. SNS collimator assembly [4].

Collimators can be used in the ring to provide the limiting apertures and thus control the location of beam losses. However, their design is not a simple matter of adding scrappers to an existing lattice. The lattice must be optimized specifically for the use of collimators. In addition, the collimator assemblies must be highly reliable and contain the activation produced by beam lost at the collimator. These features are illustrated in the collimator design for SNS shown in Figure 6 [4]. It has low Z, graphite transition pieces, water-cooling, and considerable absorber material all surrounded by iron shielding.

All of the proposed 1-5 MW spallation sources plan to use collimators. To date, it has not been possible to make effective use of scrappers or collimators at PSR because there is not enough space for them and because the lattice is not well suited to their use.

A comparison of measured (PSR 97) or expected losses from foil scattering for various rings is given in Table II below. Also shown are the parameters that are most important for determining losses from foil scattering. The parameter showing the greatest variation is the number of foil hits per stored proton which ranges from a high of ~300 for PSR in 1997 to 4-7 for the proposed next generation sources. The great improvement in expected losses for the new rings (compared with the 1997 PSR) stems largely from the small number of foil hits expected in the new rings. The larger acceptance and use of collimators also have a significant influence.

Table II. Comparison of foil scattering losses at various rings.

Ring	Foil hits /proton	Foil thickness ($\mu g/cm^2$)	Acceptance (π mm-mrad)	Collimator Acceptance (π mm mrad)	Scattering Losses %
PSR 97	300	200-220	130	NA	0.4
PSR Inj Upgrade	30	400	130	NA	0.08
SNS	4	300	312	~240	0.01
ESS	6-7	345	480	260	0.01
JHP-3GeV	3-4	200	?	312	?
SNF	?	?	530	200	?

4. Beam Losses from Field Stripping of H^0 Excited States

Foil scattering is not the only loss mechanism associated with the stripping foil. Foil stripping also leads to the production of excited states of H^0 that can field strip (via the Stark effect) part way through the magnetic fields that separate H^0, H^+ and H^- after the foil. The trajectory errors of the protons produced by field stripping can be large enough that they fall outside of the ring acceptance and are lost [5]. At PSR (1997) this mechanism accounts for a sizeable fraction (~30%) of the losses.

The yield of excited states (labeled as $H^0(n)$ where n is the principle quantum number) at 800 MeV has been measured [6]. The yield is observed to vary as $n^{-2.8}$. The lifetime of $H^0(n)$ moving in a magnetic field, B, is a strong function of n and B such that low n states are more difficult to strip. For a given B, there is a low value of n for which field stripping is negligible. For PSR at 800 MeV and a peak field of 1.2 T, the n=1 and 2 states do not strip but the higher ones ($n \geq 3$) do. For n sufficiently large, the lifetime is so short that they strip very quickly and the resulting protons stay within the ring acceptance. Thus, at PSR only the n=3,4 and 5 states lead to prompt losses. Stark states from n=5 and 6 can also add to the beam halo.

Losses from this mechanism can be mitigated by using lower magnetic fields to separate the three species emerging from the foil, by use of thicker foils to reduce the yield of $H^0(n)$ and by placing the foil in the field. The proposed rings for SNS, ESS and JHP are being designed to make optimal use of these measures to greatly reduce the expected losses from field stripping of $H^0(n)$. The experience from PSR and the expectations for the upgrade and the new rings are summarized in Table III below.

Table III. Comparison of losses from field stripping of $H^0(n)$.

Ring	Foil ($\mu g/cm^2$)	B (T)	n (loss)	Loss
PSR 1997	220	1.2	3,4,5	2.5×10^{-3}
PSR 1998	400	1.08	3,4,5	0.5×10^{-3}
SNS	300	0.25	4,5	$<10^{-6}$
ESS	345	0.177	4,5	10^{-5}
JHP	200	0.5	>4	$<8 \times 10^{-5}$

5. Stripper Foil Heating

Foil heating and radiation damage to the foil are additional consequences of charge exchange injection using stripper foils. Foil traversals by the stored beam heat the foil, which then cools by radiation primarily. Elevated temperatures are encountered which can greatly limit foil lifetime. For the 5 MW rings of the next generation spallation sources, foil heating is a serious problem. Calculated foil temperatures for various rings are shown in Table IV below.

Foil temperature depends on foil thickness, beam flux density striking the foil, foil emissivity, the number of radiating surfaces, specific heat and to a lesser extent on thermal conductivity. Foil materials in common use are graphite and aluminum oxide (Al_2O_3). Both are refractory materials with high melting or sublimation temperatures. Both are low Z materials with low Coulomb scattering cross-sections. Aluminum oxide suffers from a low emissivity, which may

rule it out for the 5 MW rings. In ESS design studies, the Al_2O_3 foil temperature is calculated to exceed the melting point.

Table IV. Calculate foil temperatures.

Ring	T(graphite) °K	T(Al_2O_3) °K
PSR 97	1780	
PSR 98	1490	
PSR/SPSS	1870	
SNS	3130	
ESS	2320	3083 (melts)

For injection schemes where the foil is placed in a magnetic field (e.g. ESS and SNS), it will be necessary to stop the stripped electrons from returning to the foil and adding to the heat load. An electron-absorbing block is placed to absorb the electrons before they return to the foil. Here it is important that the e-blocker be kept out of the way of the stored proton beam.

At PSR the commercially available foils showed a lifetime of 7-10 days in operation at 70 μA. Since changing foils entailed significant radiation dose and beam downtime, a longer lifetime foil was sought. Development of composite graphite foils by Sugai at Tokyo University has resulted in foils that lasted for ~3 months in PSR operations in 1996 and 1997 [7]. It is not known what the lifetime would be in operation at 3000 °K. This is an important R&D issue for the 5 MW rings.

6. Injection without Foils (laser-aided injection)

Given all the problems associated with the stripper foil, it would be very desirable to inject without foils. Laser stripping comes to mind as a possibility. H^0 can be efficiently produced by field stripping but photo ionization of the H^0 ground state takes a lot of short wavelength laser power and is not considered practical. In the past year, two promising new ideas have been proposed for charge-exchange injection without foils one by Y. Suzuki (JAERI) [8] and the second by I. Yamane (KEK) [9].

The layout for the Suzuki proposal is shown in Figure 7 and the profile of the undulator fields in Figure 8. His scheme makes use of a tapered undulator to strip H^- to the H^0 ground state, a laser system (ring resonator) to pump the H^0 ground state to the 3p state and a 7-period undulator (Figure 8) to ionize the 3p state. Referring to Figure 8, the laser beam pumps the H^0 ground state population to the 3p-state equilibrium population in the field-free regions and then the 3p-state population is field stripped to protons at the peak of the undulator field. This sequence is repeated 14 times in the undulator and results in a low fraction, 10^{-5}, of H^0 ground state at the exit of the undulator. The required laser power at 1062 nm is about 1 kW peak, 300 W average.

Suzuki's injection scheme was proposed for the 5 MW source at JAERI (SNF) and since then the ESS design team picked up on the idea and are developing an alternative lattice for the ESS ring using this concept. A logical next step toward development of this system would be an

experimental test with an H^- beam of around 1 GeV. Such as test is being considered, possibly with the 800 MeV H^- beam at LANSCE.

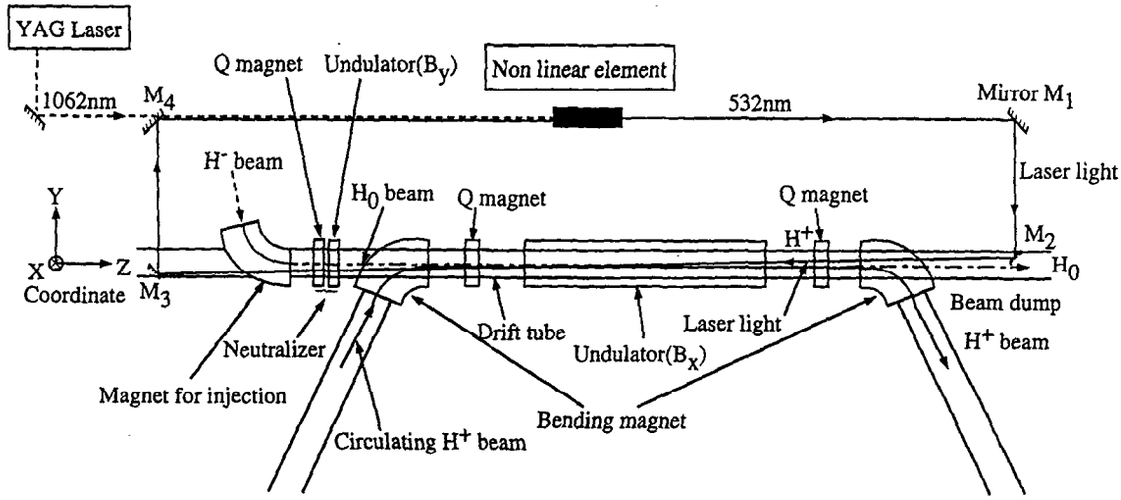

Figure 7. Layout for Suzuki's laser-aided injection system for SNF (JAERI) [8].

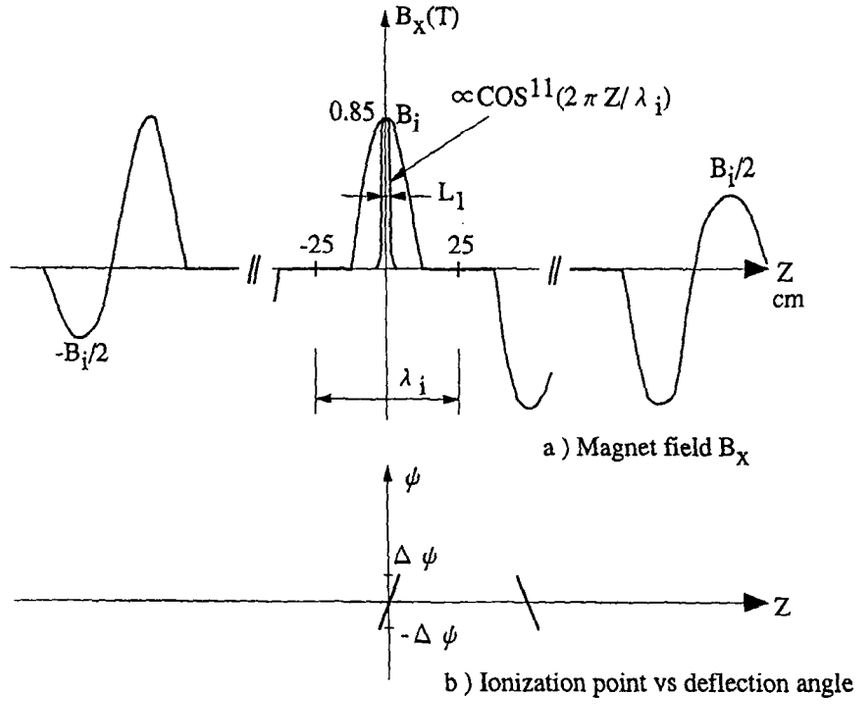

Undulator for ionizer
(λ_i=1 m, B_i=0.85 T, number of periods 7)

Figure 8. Undulator fields for Suzuki's laser-aided injection system.

The layout for another laser-aided injection system is shown in Figure 9. In Yamnane's concept nearly 100% of H^0 ground state population (obtained from Lorentz stripping H^- in a magnet) is pumped to 3p state by the optical Rabbi oscillation. The length of the collision region is chosen provide a π-phase advance of the oscillation (π pulse). The 3p state is Lorentz-stripped to

protons in another stripping magnet located at the exit of H^0-laser interaction region. There are fewer components in Yamane's concept compared to Suzuki's but the atomic and laser appears to be more delicate. Both ideas are appealing in addressing the goal of charge-exchange injection without foils.

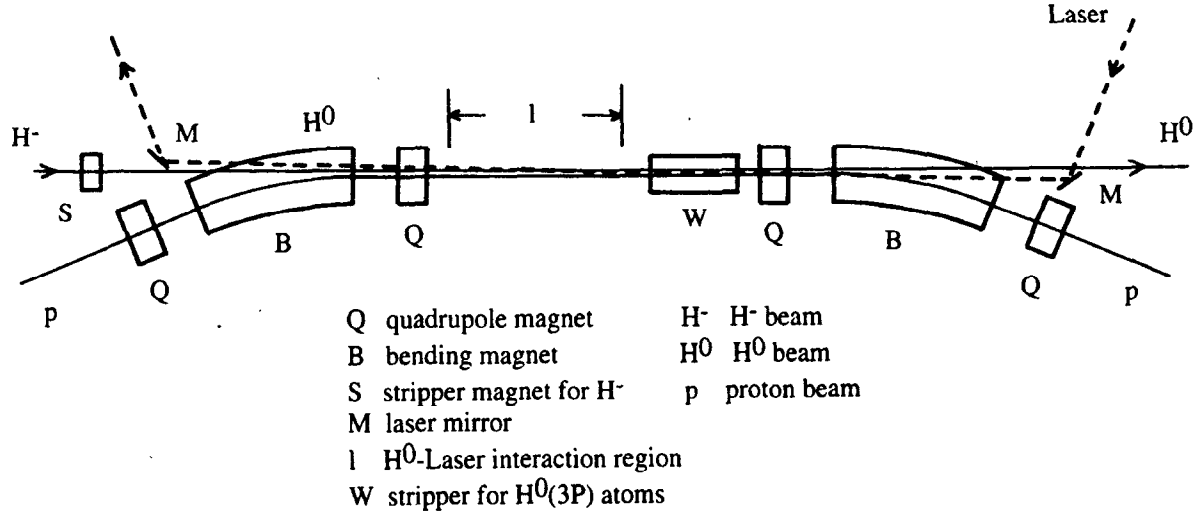

Figure 9. Layout for Yamane's laser-aided injection system [9].

7. Progress on the e-p Instability

Large and rapid beam loss from a fast instability can be a significant risk at high intensity rings. Peak intensity at PSR is limited by a strong instability that all available evidence indicates is the so-called e-p instability, which is a two-stream instability due to coupled oscillations of low energy electrons with the protons of the stored beam. In Neuffer's model, appearance of the e-p instability for a bunched beam requires both a source of electron (there are many at PSR, see Table V below) and a means of trapping some electrons during the passage of the "gap" in the bunched beam [10]. Calculations by Neuffer indicate that trapping which leads to an average beam neutralization, η, of ~1% is sufficient. His calculations also show that a small amount (<1%) of beam leaking into the gap is sufficient to trap electrons.

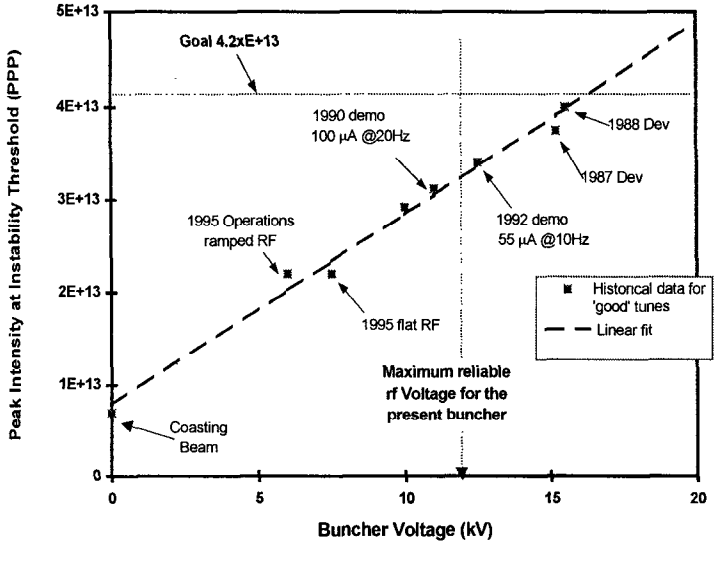

Figure 10. PSR instability threshold curve.

At PSR the stability is controlled primarily by rf voltage and proper tuning of the rf systems. The effect of the rf buncher voltage on the instability threshold intensity is shown in Figure 10. The instability shows up at ~7×10^{12} protons per pulse (PPP) for a coasting beam. The threshold

intensity increases as the buncher voltage is raised. At previous operating currents of 70 μA @ 20 Hz (2.2×10^{13} PPP) the threshold for instability was 6-8 kV (ramped). Various tests and demonstrations have carried the curve to higher intensities.

In 10 years of operating experience at PSR, much evidence has been accumulated supporting the e-p hypothesis [11]. This was discussed extensively at the Santa Fe Workshop [12]. Only the new evidence is presented here. Several experimental studies were carried out in 1997 with the goal of ensuring that the instability could be controlled to the level needed for 200 μA @ 30 Hz. The new studies included a systematic search for all the important control variables that affect the instability, further tests of the e-p hypothesis and a test of an inductive insert to passively compensate longitudinal space charge.

One of the most unambiguous predictions of Neuffer's model is the dependence of the frequency of the unstable motion on the threshold intensity, N, as shown in the following equation:

$$(2)\quad f = \frac{1}{2\pi}\sqrt{\frac{2Nr_e c^2(1-\eta_e)}{\pi b(a+b)R}}$$

Here N is the number of protons in the ring, r_e the classical radius of the electron, η_e, the average beam neutralization fraction, R, the radius of the ring , a, the vertical half size of the beam and b, the horizontal half size. The data plotted in Figure 11 show that the central frequency increases by a factor 1.4 for a factor of two increase in intensity which is in very good agreement with the expected factor of $\sqrt{2}$.

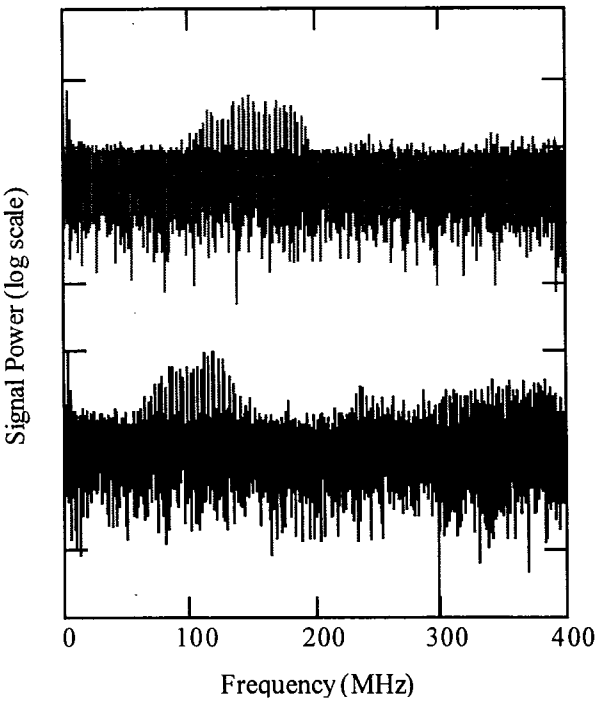

Figure 11. Frequency spectra at two beam intensities differing by a factor of 2.

The top spectrum In Figure 11 was obtained for an unstable beam with twice the intensity used for the bottom spectrum. Beam conditions for the two spectra are the same except for the beam intensity and buncher voltage. Both were taken for beams at the onset of instability.

Another expectation of the e-p model is an increase in threshold intensity as the beam size is increased. Recent measurements show that the threshold intensity increases with increasing vertical beam size.

In Neuffer's picture, a small amount of beam in the gap causes electron trapping. As a test of this idea, small but controlled amounts of beam were introduced into the gap by inhibiting chopping for a few turns of injection. As expected, the threshold was lowered as more protons were placed in the gap.

One question that is often raised is why this instability is not seen at other present day accelerators. In the past year or two there have been observations of fast instabilities at the KEK booster [13] and the CERN PS booster. It is not known if these are e-p, but it is possible.

The knowledge of the e-p instability gained at PSR has been put to good use in the design of the new machines as evidenced in the comparisons shown in Table V. The new machines, SNS and ESS, have introduced measures to greatly reduce the number of low energy electrons generated from a variety of mechanisms. In addition, the new machines will have higher rf voltage and a longer beam free gap, measures that will reduce the trapping of electrons during passage of the gap. One note of caution concerns electrons produced by beam-induced multipactor. At PSR, large numbers of electrons are suspected (but not proven) to come from beam induced multipactor. This source of electrons is not addressed in the design of the new machines.

Table V. Parameters that control the e-p instability.

Source	PSR 97	PSR 98	SNS	ESS
"Convoy" e's from H^-/H^0 stripping	1	2	blocked	blocked
Secondaries from foil	7	0.7	blocked	blocked
Secondaries from beam losses (0.1-100/lost proton	0.0006-0.6	0.00015-0.15	0.00001-0.01	0.00001-0.01
Residual gas ionization	<0.01	<0.01	<0.001	<0.0001
Beam-induced multipactor	?	?	?	?
Total	~8+?	~2.7+?	10^{-5} - 10^{-2}+?	10^{-5} - 10^{-2}+?
Length of Beam Gap (ns)	100	100	250	200
Max rf voltage/turn (kV)	12	18	40	27

8. Inductive Inserts

One of the functions of the rf system in a ring is to overcome the longitudinal space charge force which tends to push beam into the gap and thereby lowers the e-p instability threshold. The net voltage per turn, V_s, from space charge self-voltage and inductive wall impedance (below transition) is given by:

$$(3)\quad V_s = \frac{\partial\lambda(s)}{\partial s}\left[\frac{g_0 Z_0}{2\beta\gamma^2} - \Omega_0 L\right] e\beta c R$$

Here $\lambda(s)$ is the line density of charge, $g_0 = 1 + 2\ln(b/a)$, b the vacuum pipe radius, a the beam radius, $Z_0 = 377$ ohms, Ω_0 the angular frequency of revolution, L the wall inductance and R the mean radius of the ring. The idea of the inductive insert is to add sufficient ferrite to increase L until V_s vanishes.

Inductor tests at PSR carried out by a LANL and FNAL collaboration [14] had three main goals:

- provide a check on space charge compensation;
- measure the effect of the inductor on the PSR instability threshold and
- check that the inductor has no unexpected, deleterious effects on the ring operation.

During the 3-day test with the inductor in place, no unusual problems arose in the operation of the ring that could be attributed to the inductor. A check on space charge compensation was made by measuring the bunch broadening for a narrow (50 ns) pulse and comparing to simulations. The effect was not large but it was reproducible and agreed with the ACCSIM simulations.

The effect of the inductive insert on the e-p instability was studied by measuring the threshold intensity as a function of buncher rf voltage. The results are plotted in Figure 12 along with historical data and other 1997 data. The highest intensity point of the inductor data (triangle symbols) lies to the left of the historical trend line and indicates that less rf voltage was needed to keep the beam stable. However, it is not possible to draw a strong conclusion since other points, not involving the inductor, also lie to the left of the trend line. It is perhaps fair to say that the highest intensity point shows a two-standard deviation effect, which is encouraging but not conclusive or definitive. The effect would be more convincing if contemporaneous measurements of the threshold curve were made with the inductor at full its maximum value and another at a low value. Time ran out before this could be done.

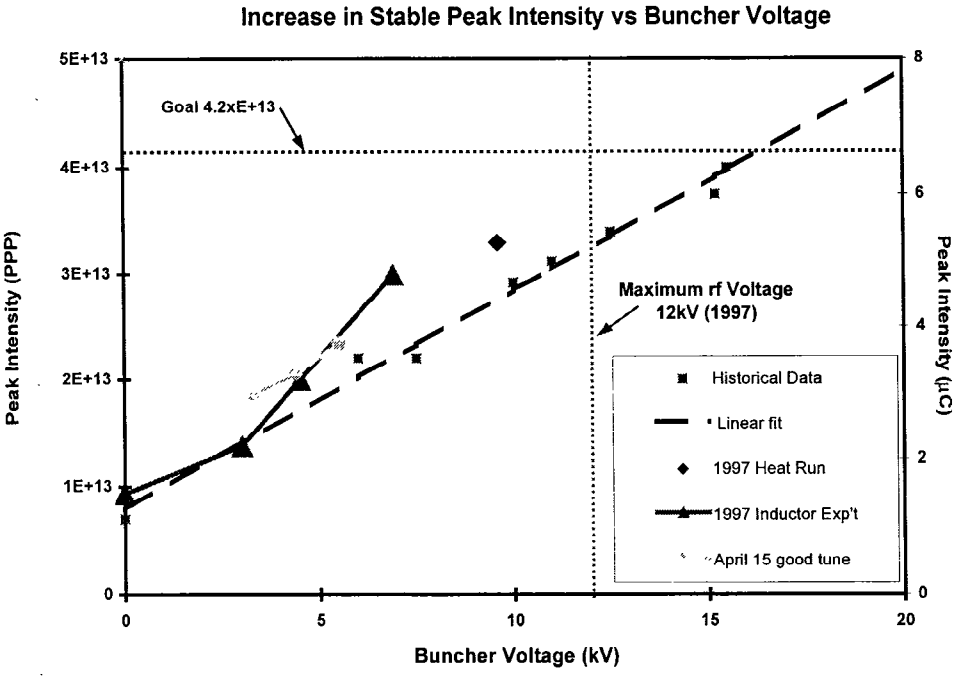

Figure 12. Effect of an inductor on the PSR instability threshold curve.

9. Conclusions

The advent of the new projects for 1-5 MW short pulse sources and other high intensity proton rings has prompted new work on intensity limitations in proton rings and new work on the technologies needed for high intensity. Good, incremental progress has been made in some areas and good beginnings in others. From today's perspective the major issues for the immediate future are the peak intensity from the ion-source and linac (not discussed here), beam losses in the ring, the e-p instability and stripper foil technology.

The PSR has proven to be a good test bed for the linac-accumulator ring option. Its operation has identified important problems that need to be solved for the next generation rings. It is important for future accumulators to fully understand the PSR instability and means to control it.

The recent ideas for laser injection that eliminate the need for stripper foils are quite appealing. However, it is too early in their development to predict the final outcome

10. References

[1] R. Baartman, "Betatron Resonances with Space Charge Due to Self-Fields", Proceedings of Workshop on Space Charge Physics in High Intensity Hadron Rings, May 4-7, 1998, Pridwin Hotel, Shelter Island, Long Island, to be published.

[2] Sessions on simulations, Proceedings of Workshop on Space Charge Physics in High Intensity Hadron Rings, May 4-7, 1998, Pridwin Hotel, Shelter Island, Long Island, to be published.

[3] J Galombus, private communication.

[4] SNS Design manual, June 1998, p 5-98.

[5] R. Hutson and R. Macek, "First Turn Losses in the LANSCE Proton Storage Ring", Proceedings of the 1993 Particle Accelerator Conference, p. 363, 1993.

[6] M. Gulley et al, "Measurement of H^-, H^0 and H^+ yields produced by foil stripping of 800-MeV H^- ions", Phys. Rev. A53 (1996), p 3201-10.

[7] I. Sugai et al, "Development of thick, long-lived carbon stripper foils for PSR of LANL", NIM A 363 (1995) p 70-76.

[8] Y. Suzuki, private communication.

[9] I. Yamane, "A new scheme for H^- charge exchange injection without hazardous stripping foils", KEK Prepring 98-42, May 1998, to be published in Physical Review Special Topics: Accelerators and Beams.

[10] D. Neuffer et al, "Observations of a fast transverse instability in the PSR", NIM A321 (1992), p 1-12.

[11] M. A. Plum et al, "Recent Experimental Evidence for the Los Alamos Proton Storage Ring Instability", Proceedings of the 1997 Particle Accelerator Conference, 12-16 May 1997, Vancouver, BC, Canada, to be published.

[12] Proceedings of the Santa Fe Workshop on Electron Effects, March 5-7, 1997, LANL report, LA-UR-98-1601.

[13] Y. Irie et al, "Electron-Proton or Ion-Oscillation-Like Instabilities in the KEK Booster Synchrotron", Proceedings of the International Workshop on Multibunch Instabilities in Future Electron and Positron Accelerators, July 15-18, 1997 KEK, Tsukuba, Japan, p 247-255.

[14] M. A. Plum et al, "Experimental Study of Passive Compensation of Space Charge Potential Well Distortion at the LANL Proton Storage Ring", PSR Tech note 98-013, April 1998.